International Journal of GEOMATE, Sep., 2025 Vol.29, Issue 133, pp. 81-88
ISSN: 2186-2982 (P), 2186-2990 (O), Japan, DOI: https://doi.org/10.21660/2025.133.5023
Geotechnique, Construction Materials and Environment

POST-BUCKLING BEHAVIOR OF COLD-FORMED STEEL SQUARE PLATE FIXED SUPPORTED UNDER PURE SHEAR

*Arif Sandjaya[1], Sofia Wangsadinata Alisjahbana[2], Bambang Suryoatmono[3] and Andy Prabowo[1]

[1]Department of Civil Engineering, Universitas Tarumanagara, Indonesia; [2]Civil Engineering, Bakrie University, Indonesia; [3]Department of Civil Engineering, Parahyangan Catholic University, Indonesia

*Corresponding Author, Received: 21 April 2025, Revised: 23 June 2025, Accepted: 26 June 2025

ABSTRACT: The ability to resist loads after experiencing elastic buckling is post-buckling strength, an important factor in the design and analysis of thin-walled structures. Many models are based on tension field actions, which state that the main source of post-buckling strength is the development of tensile stresses in certain diagonal planes. Post-buckling behavior has been extensively investigated in hot-rolled steels for a long time; however, it has not been extensively studied in cold-formed steels (CFS). This study presents experimental and finite element models for pure shear from CFS, namely Galvanized 550, with thicknesses of 0.5 mm and 0.7 mm. An experimental test using a square plate clamped on each side. The plate is placed at a 45-degree angle and then pressed. The clamp will transmit force to the plate like shear. A finite element model using Abaqus, where the plate is on the XY plane, where displacement Z and X, Y, Z rotations are 0. The results of this study show that the first compressive stress appears at the corner, but the compressive stress continues to increase towards the middle of the diagonal. The developed finite element model gives conservative shear load results. The deformation of the finite element model gives the same shape as the experimental test. These findings can help better understand the post-buckling behavior and show a finite element model that is easy to apply.

Keywords: Post-buckling, tension field actions, cold-formed steel, pure shear

1. INTRODUCTION

Cold-formed steel (CFS) began to be used in building construction around 1850 in the United States and England. However, it did not become widely used until about 1940. Since 1946, the use and development of thin-walled steel construction in the United States have been accelerated by the publication of several editions of the Specification for the design of CFS structural members from the American Iron and Steel Institute (AISI). CFS designs at that time were still largely based on hot-rolled steel (HRS). Because CFS structural elements are usually made of light-gage steel and have different geometric shapes than HRS, the behavior and performance of loaded CFS structural elements differ in some important respects from HRS structures [1].

Steel plates with a high width-to-thickness ratio (thin-walled) are commonly used in steel construction, such as steel plate shear walls (SPSW). Shear strength is usually the determining factor in the capabilities of thin-walled designs. Plates that buckle elastically under shear loading still have significant post-buckling shear strength. This post-buckling behavior has attracted the attention of researchers and engineers. Many publications that make post-buckling models are based on tension field action. Tension field theory states that the main source of this post-buckling shear strength is the development of tensile stresses in certain diagonal planes [2].

Glassman and Garlock [3] found the earliest recorded explanation for the post-buckling shear strength of a girder web with stiffeners by J. M. Wilson in 1886, assuming that the transverse stiffeners acted like the trusses of a Pratt truss, with the web subjected to diagonal tensile stresses. However, researchers have found that the large axial loads expected in the transverse stiffeners due to their resistance of the diagonal tensile fields are smaller than expected for the assumed truss action.

Wagner [4] stated that after elastic shear buckling occurs in the web, the compressive stress does not increase, and additional shear strength (post-buckling) occurs due to the formation of diagonal tensile stresses. However, the assumption that compressive stress does not increase in the post-buckling range has been proven to be inaccurate based on the findings of many authors using finite element analysis. Tensile fields do form, compression is always the catalyst for buckling, and many assumptions inherent in the tensile field theory have since been proven to be inaccurate.

The larger the out-of-plane deformation, the smaller the axial stiffness. Therefore, the stress does not increase much (or at all) near the center after elastic buckling. The out-of-plane deformation is much smaller at the corners, causing the stress to continue to increase after elastic buckling [3]. Diagonal compressive stress continues to increase near the panel edges after buckling, which is contrary to the fundamental assumption adopted [5].

Research that states pure shear but takes part of the web girder is not the same as pure shear, because

there is bending simultaneously. For example, research on post-buckling mechanics of rectangular slender steel plates under pure shear force on the plate for ordinary steel girder highway bridges. The finite element model using the simply supported boundary conditions shown in Fig. 1 and Table 1. To achieve perfect symmetric stress results, boundary conditions are created to restrain the Y translation on the left side instead of applying a load [2]. The plates are on the Y and Z planes. This assumption also does not show the presence of girder flanges well (Fig. 2), where the upper flange will experience tension and the lower flange will experience compression.

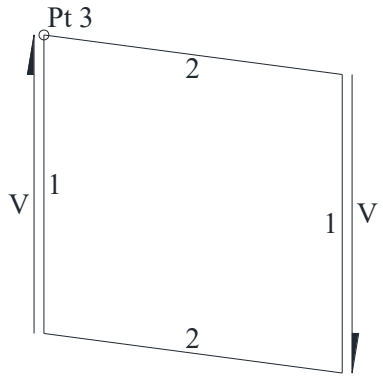

Fig. 1 Naming the location (1, 2, Pt 3), direction of shear force (V), and changes in plate shape [2]

Table 1. Boundary conditions of the finite element model

	1	2	Pt 3
Ux	0	0	0
Uy	Free	Free	0
Uz	0	0	0
Rx	0	0	0
Ry	Free	0	0
Rz	0	Free	0

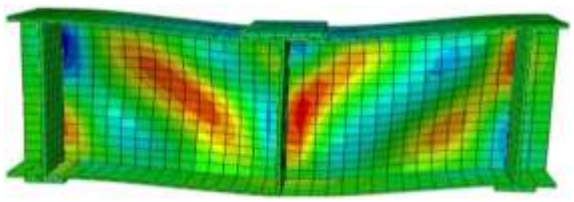

Fig. 2 Stresses distribution and failure modes for flat web with ratio width/height panel = 1 [6]

Pure shear stress occurs in an element as shown in Fig. 3a, the shear stress that works will change the shape of the element as illustrated in Fig. 3b [7]. Notice the top left and bottom right corner points move, causing them to move closer together and eventually meet. Meanwhile, the point in the upper right corner moves away from the point in the lower left corner. The side length of the element does not change. Compared to Fig. 1, the difference is that side number 1 will move exactly vertically, so the distance between them will always be the same, and the length of side number 2 will be longer.

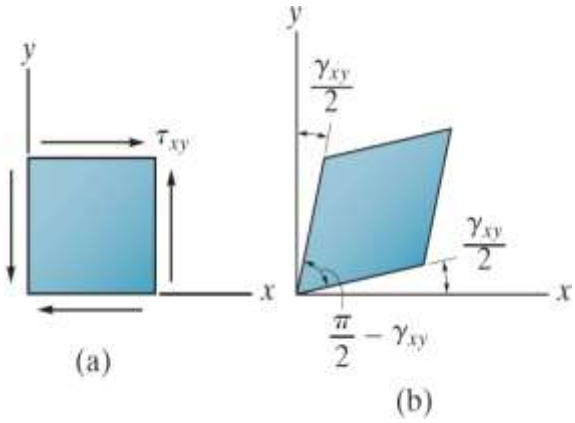

Fig. 3 Illustration of element (a) given shear stress and (b) changing shape due to shear stress [7]

A conventional steel-plate shear wall (SPSW) is constrained by a boundary frame consisting of vertical and horizontal structural members. The steel plate buckles under low shear loads with the formation of a diagonal tension field, which is a mechanism that allows it to withstand further lateral forces [8]. Imagine the portal collapsing, it would be like Fig. 3b until all sides become 1 line.

Unmodified SPSW can perform well on tension field action. Stiffened SPSW increases buckling strength and change tension field formation [9]. Rectangular openings in the SPSW (with approximately the same area) cause irregularities in the displacement, possibly because the position of the opening disturbs the action of the tensile field [10].

The theoretical equation research for the shear strength of double-sided clamped SPSW [7] may be close to the assumptions in Fig. 1, but is only valid if the deformation that occurs is small.

Researchers were initially pessimistic that direct experimental verification of the pure diagonal tensile stress theory would be impossible [9]. Simulation of pure shear stress acting on a steel plate can be done by rotating it 45 degrees, clamping it in a frame on each side, and applying a compressive load (Fig. 4). The compressive load applied to the clamping plate generates a shear load that is distributed uniformly along the edges of the steel test plate through the bolts [10].

This study will present how to construct a simple finite element model for pure shear, its compatibility with experimental tests, and the post-buckling behavior of CFS. This simple model is expected to be a reference for SPSW modeling.

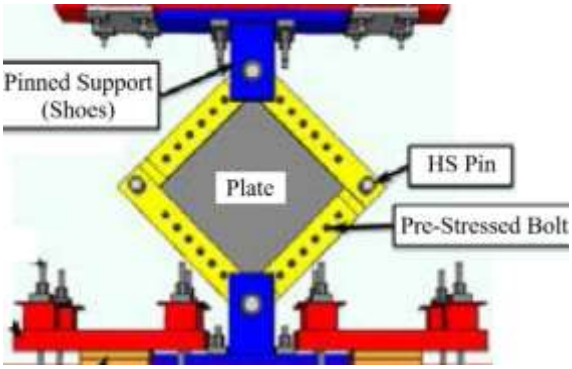

Fig. 4 Illustration of pure shear test method [10]

2. RESEARCH SIGNIFICANCE

Current post-buckling strength design is still based on assumptions that do not follow the actual behavior. This study presents the behavior of a cold-formed steel plate subjected to pure shear and creates a simple finite element model that closely resembles reality. The compressive stress continues to increase at the corners and continues to spread to the center of the plate. The stages of tensile stress are also formed flanking the compressive stress. This causes the work of the tensile field action on the plate to be wider in the middle compared to that described by the theory, which is considered straight from the corner.

3. RESEARCH METHODS

3.1 Experimental Method

The square steel plate used is Galvanized 550 with a side size of 151 mm. The thickness of the plate is 0.5 and 0.7 mm to see the influence of thickness. The test object model follows the concept of Fig. 4. The clamping frame and supports are made of 6 mm thick and 24 mm wide aluminum to reduce the effect of self-weight. The bolts used have a diameter (d) of 6 mm.

The hole positions are arranged according to AISI S100-16 rules [11]. Fig. 5 shows that the minimum distance to the edge is 1.5d (12 mm) and the distance between bolts is 3d (18 mm). The holes in the corners are spaced further apart (27.5 mm) to provide sufficient clearance for the stacked clamping frames and supports. Each corner hole uses a bearing pin to allow it to rotate freely. The longer bearing pin is used as support to prevent it from contacting the bolt. The layout plan for the clamping frame can be seen in Fig. 6. The results of the test object assembly are shown on Fig. 7.

3.2 Finite Element Method

Finite element model analysis using Abaqus. The model size is the same as the free plate that is not clamped by the frame, which is 103 mm. Assuming the plate is on the XY plane, the confined boundary conditions for each side are the Z displacement and the X, Y, Z rotations. Model using shell elements and quadrilateral (S4R) meshing of 1 mm. Linear analysis or elastic buckling is performed by giving a shear load on each side of 1 unit and the direction follows Fig. 3a. Nonlinear or post-buckling analysis is performed by giving a displacement of 5 mm on each side in the direction following Fig. 3a. The magnitude of the displacement is taken from the diagonal extension of the experimental test obtained. An illustration of the model created can be seen in Fig. 8. The plate will be stable by providing balanced shear loads and displacement.

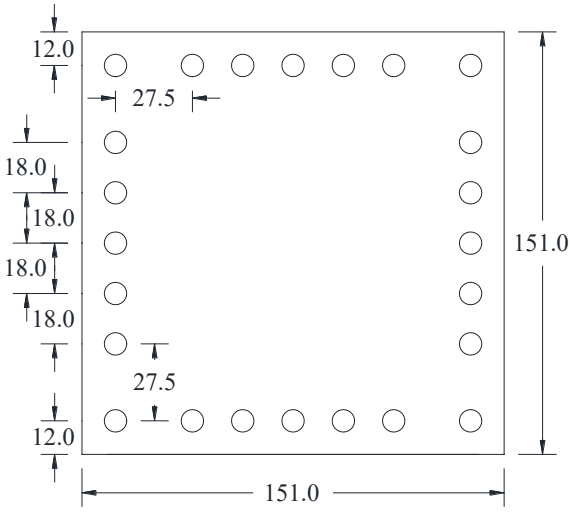

Fig. 5 Size and location of holes for plate test objects (mm).

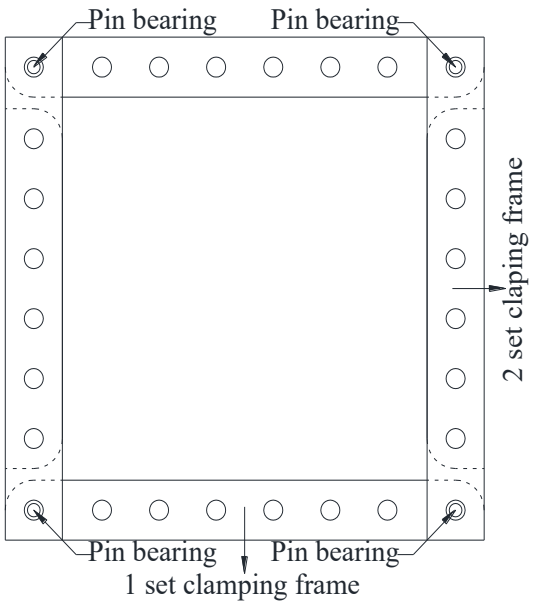

Fig. 6 Clamping frame position

Fig. 7 Pure shear plate test specimen

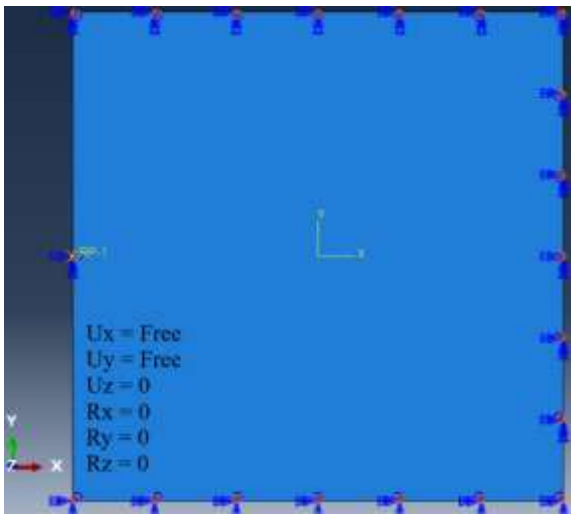

Fig. 8 Boundary condition each side of plate

4. RESULTS AND DISCUSSIONS

Fig. 9 shows the results of a 0.5 mm thick plate compression test. The average compressive load is 16.23 kN. The shear load received by the plate is the distribution of the compressive load to the left-right clamping frame and is angled at 45 degrees. The shear load of the plate becomes 11.48 kN. This angle will continue to change along with the vertical displacement that occurs. In this case, it is ignored because the displacement is not large compared to the diagonal length of the plate (<10%).

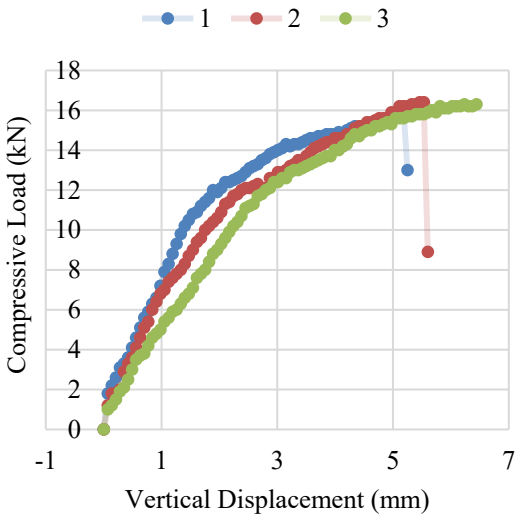

Fig. 9 Graph of compressive load and vertical displacement of 3 test plates with a thickness of 0.5 mm

The visual condition of the plate after the test is represented in Fig. 10, where the largest out-of-plane displacement is in the center of the plate.

Fig. 10 Representative conditions after 0.5 mm thick plate test

Fig. 11 shows the results of a 0.7 mm thick plate compression test. The average compressive load is 23.67 kN. The shear load of the plate becomes 16.73 kN.

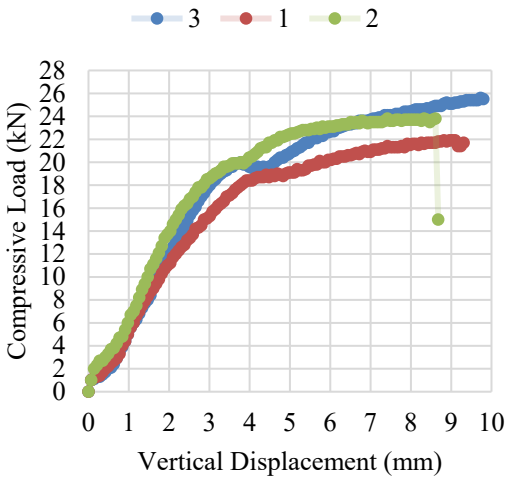

Fig. 11 Graph of compressive load and vertical displacement of 3 test plates with a thickness of 0.7 mm

The visual condition of the plate after the test is represented in Fig. 12, where the largest out-of-plane displacement is in the center of the plate.

Fig. 12 Representative conditions after 0.7 mm thick plate test

The results of linear shear buckling mode 1 of a plate with a thickness of 0.5 mm are shown in Fig. 13. The nonlinear (post-buckling) loads and deformations are shown in Fig. 14. The highest load (Vu) is 7.60 kN.

Fig. 15 shows the results of Von-Mises stress at Vu, where the red color indicates that the stress has exceeded Fy (Min 550 MPa). Fig. 16 shows the results of the maximum principal stress at Vu, where the red color indicates tensile stress and the blue color indicates compression. The tensile stress has exceeded Fy, but the compressive stress has not exceeded Fy. Fig. 17 shows the results of the minimum principal stress at Vu. The tensile stress has not exceeded Fy, but the compressive stress has exceeded Fy.

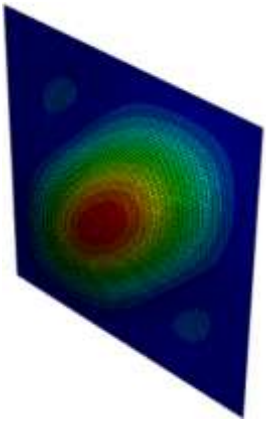

Fig. 13 Mode 1 from plate with a thickness of 0.5 mm

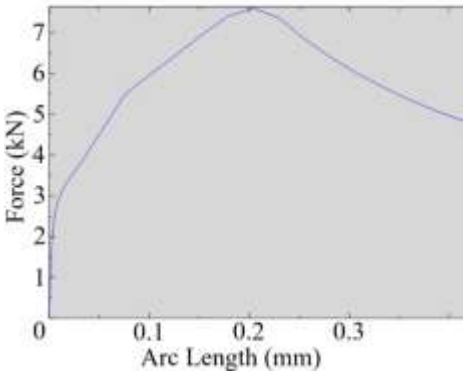

Fig. 14 Graph of force and arc length of 0.5 mm thick plate

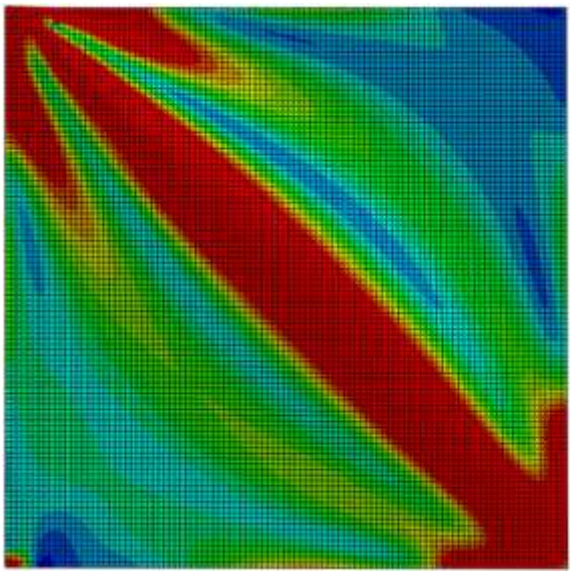

Fig. 15 Von-Mises stress contour of 0.5 mm plate at Vu

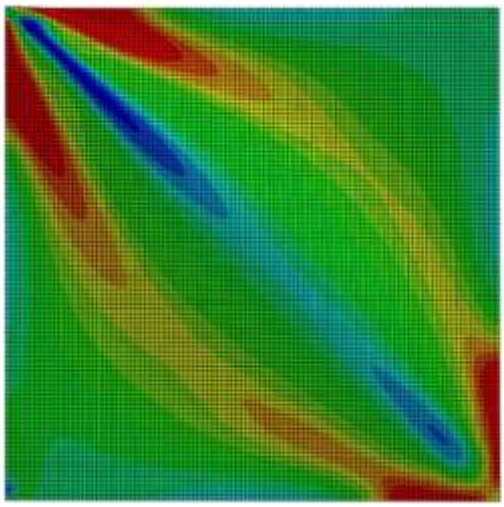

Fig. 16 Maximum principal stress contour of 0.5 mm plate at Vu

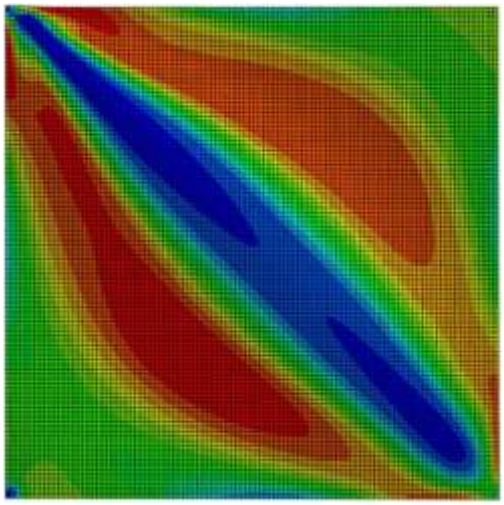

Fig. 17 Minimum principal stress contour of 0.5 mm plate at Vu

Fig. 18 shows the results of plate deformation after passing through Vu, where the results are similar to the experimental test.

The results of linear shear buckling mode 1 of a plate with a thickness of 0.7 mm are shown in Fig. 19. The nonlinear (post-buckling) loads and deformations are shown in Fig. 20. The highest load (Vu) is 13.70 kN. Fig. 21 shows the results of Von-Mises stress at Vu, where the red color indicates that the stress has exceeded Fy. Fig. 22 shows the results of the maximum principal stress at Vu, where the red color indicates tensile stress and the blue color indicates compression. The tensile stress has exceeded Fy, but the compressive stress has not exceeded Fy. Fig. 23 shows the results of the minimum principal stress at Vu. The tensile stress has not exceeded Fy, but the compressive stress has exceeded Fy.

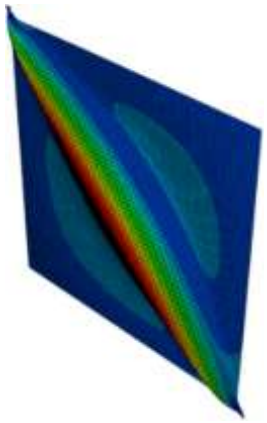

Fig. 18 The result of 0.5 mm plate deformation after passing through Vu.

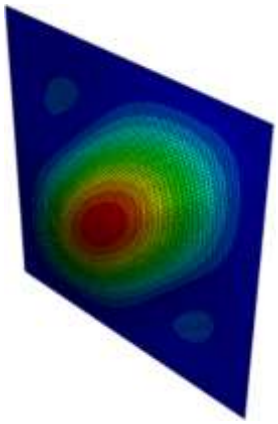

Fig. 19 Mode 1 from plate with a thickness of 0.7 mm

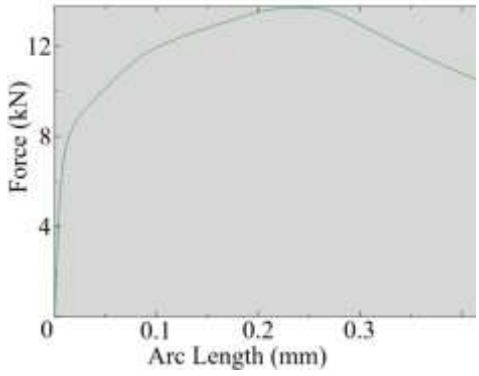

Fig. 20 Graph of force and arc length of 0.7 mm thick plate

Fig. 24 shows the results of plate deformation after passing through Vu, where the results are similar to the experimental test.

The shear load from the experimental test was greater than that from the finite element method for both plate thickness tested. The Vu of the 0.5 mm thick plate is 33.80% lower (11.48 kN > 7.60 kN). The Vu of the 0.7 mm thick plate is 18.11% lower (16.73 kN > 13.70 kN). This is because the thickness

of the experimental test plate can be thicker. For example, a plate thickness of 0.5 mm can be found to be 0.5~0.6 when measured with a caliper on all four sides of the plate.

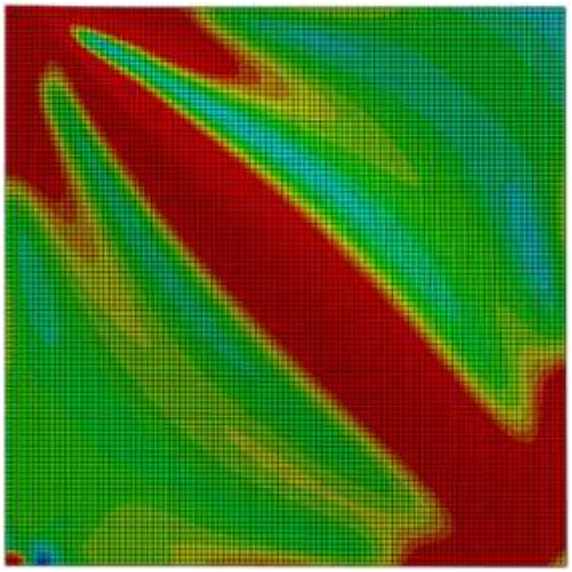

Fig. 21 Von-Mises stress contour of 0.7 mm plate at Vu

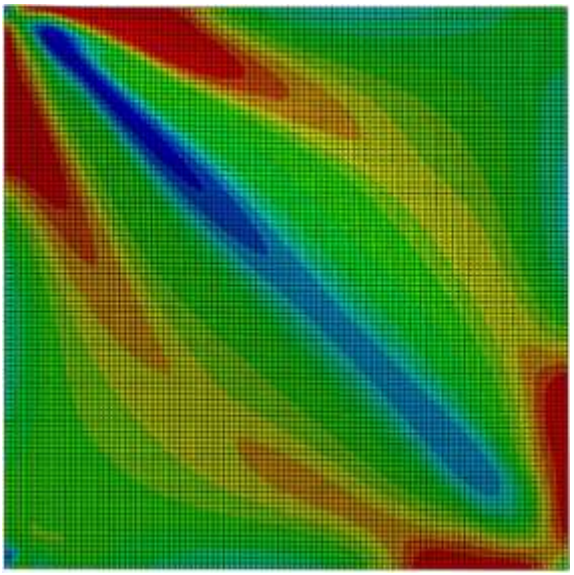

Fig. 22 Maximum principal stress contour of 0.7 mm plate at Vu

The shape changes of the plate after passing through Vu between the experimental test and the finite element method are similar. By pulling diagonally at both ends of a 7.07 mm thick plate, the 0.5 mm thick plate experiences out-of-plane buckling of 7.8 mm, and the 0.7 mm thick plate experiences out-of-plane buckling of 6.6 mm.

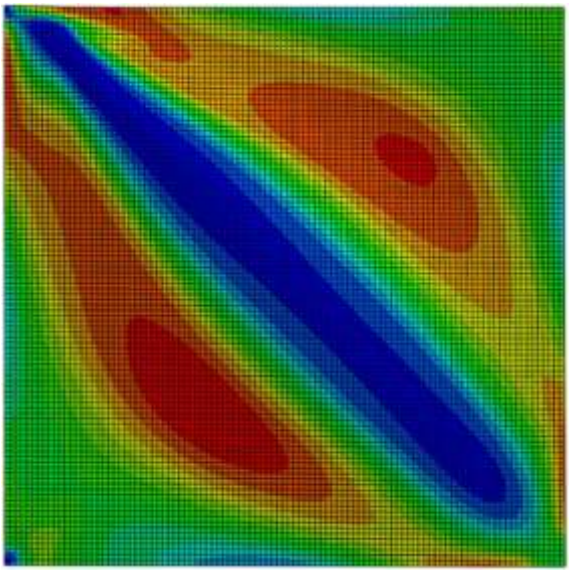

Fig. 23 Minimum principal stress contour of 0.7 mm plate at Vu

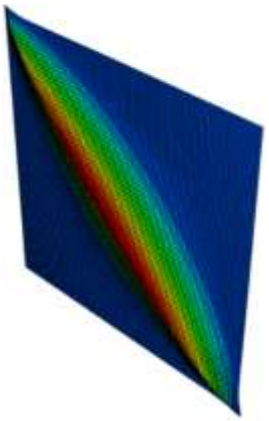

Fig. 24 The result of 0.7 mm plate deformation after passing through Vu.

5. CONCLUSIONS

The results of the study show that the diagonal compressive stress not only continues to increase near the edge of the panel after buckling but also increases towards the center of the panel.

The principal stress distribution stage during post-buckling begins with the emergence of a pair of tensile stresses from two areas near the corners of the plate. Then, compressive stresses appear near the ends between the tensile stresses. This compressive stress causes the plate to bend out of the plane, starting from the corner in the diagonal direction. Both tensile and compressive stresses will spread toward the center of the plate (diagonally), so that the highest stress is at the end corners of the plate, not in the middle.

Vu from the results of finite element model

analysis, which is smaller than the experimental test (18% for 0.7 mm thickness and 33% for 0.5 mm thickness), can be seen as conservative and safe to use.

The similarity of the plate shape changes (square to parallelogram and out of plane) from the finite element model can increase the confidence that the assumed boundary conditions are close to the actual plate conditions.

By observing the stress process that is formed, it can provide information for adding efficient stiffeners.

6. REFERENCES

[1] Yu W.W. and LaBoube R.A., Cold-Formed Steel Design, Canada, John Wiley & Sons, Inc., 2010, pp. 1-491.

[2] Garlock M.E.M., Quiel S.E., Wang P.Y., Alós-Moya J., and Glassman J.D., Post-Buckling Mechanics of a Square Slender Steel Plate in Pure Shear, Engineering Journal, Vol. 56, 2019, pp. 27-46.

[3] Glassman J.D. and Garlock M.E.M., A Compression Model for Ultimate Postbuckling Shear Strength, Thin-Walled Structure, Vol. 102, 2016, pp. 258-272.

[4] Wagner H., Flat Sheet Metal Girders with Very Thin Metal Web (Part 1, General Theories and Assumtions), National Technical Information Service, 1931, pp. 1-43.

[5] Yoo C.H. and Lee S.C., Mechanics of Web Panel Postbuckling Behavior in Shear, Journal of Structural Engineering, Vol. 132, Issue 10, 2006, pp. 1580-1589.

[6] Muhaisin M.H., Kadhim H.A., Mohammed K.A., Ammash H.K. and Hussein Z.H., Numerical Investigation of Plate Girder Having Core Web with Zigzag Corrugated Panel, International Journal of GEOMATE, Vol. 25, Issue 110, 2023, pp. 251-258.

[7] Hibbeler R.C., Mechanics of Materials (8th ed.), New York, Prentice Hall, 2011, pp. 1-862.

[8] Shin D.H. and Kim H.J., Post-Buckling Strengths of Steel-Plate Shear Walls with Two-Side Clamped Boundary Conditions, Thin-Walled Structures, Vol. 170, 2022, pp. 108499.

[9] Zhou N., Xiong F., Huang Q.Y., Ge Q., and Chen J., Literature Review of Seismic Behavior of Composite Steel Plate Shear Wall, Advanced Materials Research, Vol. 671-674, 2013, pp. 1408-1413.

[10] Ibrahim I., Shakor P., Qader D.N., Al-Luhybi A.S., and Sathvik, A Comprehensive Review of Recent Experimental and Numerical Investigations on the Impact of Openings in Steel Plate Shear Walls (SPSWs), Passer Journal, Vol. 6, Issue 2, 2024, pp. 275-285.

[11] Kuhn P., Peterson J.P. and Levin L.R., A Summary of Diagonal Tension Part 1 - Methods of Analysis, Washington, National Advisory Committee for Aeronautics, 1952, pp. 1-131.

[12] Kazem H., Rizkalla S., Seracino R. and Kobayashi A., Small-Diameter CFRP Strands for Strengthening Steel Bridge Girder, In the 12th International Symposium on Fiber Reinforced Polymers for Reinforced Concrete Structures & The 5th Asia-Pacific Conference on Fiber Reinforced Polymers in Structures, Nanjing, 2015, pp. 1-7.

[13] American Iron and Steel Institute, North American Specification for the Design of Cold-Formed Steel Structural Members (AISI S100), Mexico, Canacero, 2016, pp. 1-137.